Astron. Astrophys. 315, L38–L42 (1996)

ASTRONOMY AND ASTROPHYSICS

The ISO Long-Wavelength Spectrometer⋆

P.E. Clegg[1], P.A.R. Ade[1], C. Armand[2], J.-P. Baluteau[3,4], M.J. Barlow[5], M.A. Buckley[6], J.-C. Berges[3], M. Burgdorf[2], E. Caux[7], C. Ceccarelli[8], R. Cerulli[8], S.E. Church[9], F. Cotin[7], P. Cox[10,19], P. Cruvellier[3], J.L. Culhane[11], G.R. Davis[12], A. Di Giorgio[2], B.R. Diplock[6], D.L. Drummond[6], R.J. Emery[6], J.D. Ewart[2], J. Fischer[13], I. Furniss[5], W.M. Glencross[5], M.A. Greenhouse[14], M.J. Griffin[1], C. Gry[2,3], A.S. Harwood[6], A.S. Hazell[1], M. Joubert[3,15], K.J. King[6], T. Lim[2], R. Liseau[8,16], J.A. Long[6], D. Lorenzetti[17], S. Molinari[2], A.G. Murray[1], D.A. Naylor[18], B. Nisini[8], K. Norman[11], A. Omont[19], R. Orfei[8], T.J. Patrick[11], D. Péquignot[20], D. Pouliquen[3], M.C. Price[2], Nguyen-Q-Rieu[21], A.J. Rogers[6], F.D. Robinson[22], M. Saisse[3], P. Saraceno[8], G. Serra[7], S.D. Sidher[2], A.F. Smith[6], H.A. Smith[14], L. Spinoglio[8], B.M. Swinyard[6], D. Texier[2], W.A. Towlson[5], N.R. Trams[2], S.J. Unger[6], and G.J. White[1]

[1] Queen Mary and Westfield College, University of London, Mile End Road, London E1 4NS, UK
[2] The LWS Instrument-Dedicated Team, ISO Science Operations Centre, PO Box 50727, E-28080 Madrid, Spain
[3] Laboratoire d'Astronomie Spatiale, CNRS, BP 8, F-13376 Marseille Cedex 12, France
[4] Observatoire de Marseille, 2 place de Verrier, F-13248 Marseille, France
[5] Department of Physics and Astronomy, University College London, Gower Street, London WC1E 6BT, UK
[6] Rutherford Appleton Laboratory, Chilton, Didcot, Oxon OX11 0QX, UK
[7] Centre d'Etude Spatiale des Rayonnements, CNRS, 9 avenue de Colonel Roche, F-31029 Toulouse, France
[8] CNR-Istituto de Fisica dello Spazio Interplanetario, CP 27, I-00044 Frascati, Italy
[9] Observational Cosmology, MC 59-33, California Institute of Technology, Pasadena, CA 91125, USA
[10] Institut d'Astrophysique Spatiale, Bâtiment 120, Université de Paris XI, F-91405 Orsay, France
[11] Mullard Space Science Laboratory, University College London, Holmbury St Mary, Dorking, Surrey RH5 6NT, UK
[12] Institute of Space and Atmospheric Studies, University of Saskatchewan, Saskatoon, Saskatchewan, S7N 5E2, Canada
[13] Naval Research Laboratory, Remote Sensing Division, 4555 Overlook Avenue SW, Washington, DC 20375, USA
[14] National Air and Space Museum, Smithsonian Institution, Laboratory for Astrophysics, Washington, DC 20560, USA
[15] CNES, 2 Place Maurice Quentin, F-75001 Paris, France
[16] Stockholm Observatory, S-133 36 Saltsjöbaden, Sweden
[17] Osservatorio Astronomico di Roma, I-00040 Monte Porzio, Italy
[18] Department of Physics, University of Lethbridge, 4401 University Drive, Lethbridge, Alberta, T1K 3M4, Canada
[19] Institut d'Astrophysique de Paris, CNRS, 98bis boulevard Arago, F-75014 Paris, France
[20] Observatoire de Paris Meudon, Place Janssen, F-92190 Meudon, France
[21] Observatoire de Paris, 61 avenue de l'Observatoire, F-75014 Paris, France
[22] Code 717.3, NASA Goddard SFC, Greenbelt, MD 20771, USA

Received 5 August 1996 / Accepted 22 August 1996

Abstract. The Long-Wavelength Spectrometer (LWS) is one of two complementary spectrometers aboard the European Space Agency's Infrared Space Observatory[1] (ISO) (Kessler et al., 1996). It operates over the wavelength range 43 – 196.9 μm at either medium (about 150 to 200) or high (6800 to 9700) spectral resolving power. This Letter describes the instrument and its modes of operation; a companion paper (Swinyard et al, 1996) describes its performance and calibration.

Key words: artificial satellites, space probes – instrumentation: spectrographs – infrared: general

1. Introduction

Astronomical observations at far-infrared wavelengths, from about 20 μm to 300 μm, are almost impossible from the ground because of atmospheric emission and absorption. Even at aeroplane and balloon altitudes, spectroscopy is difficult because telluric lines obscure weaker and narrower extra-terrestrial lines. The LWS covers the almost unexplored wavelength range 43 – 196.9 μm: the shorter wavelength end overlaps with the 2.5 – 45 μm range of the Short-Wavelength Spectrometer (de

Send offprint requests to: P.E. Clegg (p.e.clegg@qmw.ac.uk)

⋆ ISO is an ESA project with instruments funded by ESA Member States (especially the PI countries: France Germany, the Netherlands and the United Kingdom) and with the participation of ISAS and NASA.

Graauw et al., 1996) whilst the longest wavelength is close to the current limit for photoconductive detectors.

The LWS was designed to achieve the two main objectives of astronomical spectroscopy: the detection and identification of dust (or solid state) features and lines - together with a determination of their strengths and ratios - for which moderate spectral resolving power often suffices; and the study of the shapes of lines for kinematic purposes, for which high resolving power is needed. [High resolving power is also needed to detect very faint lines sitting on a strong continuum.] We therefore chose to design the LWS to operate in two modes. In its moderate-resolution mode, its spectral resolution element is 0.29μm between 43 μm and 94.6 μm and 0.60 μm between 94.6 μm and 196.9 μm. In high-resolution mode, its resolving power varies between 8100 and 8500, for the wavelength range $47 - 70$ μm, and between 6800 and 9700 for the wavelength range $70 - 196.6$ μm.

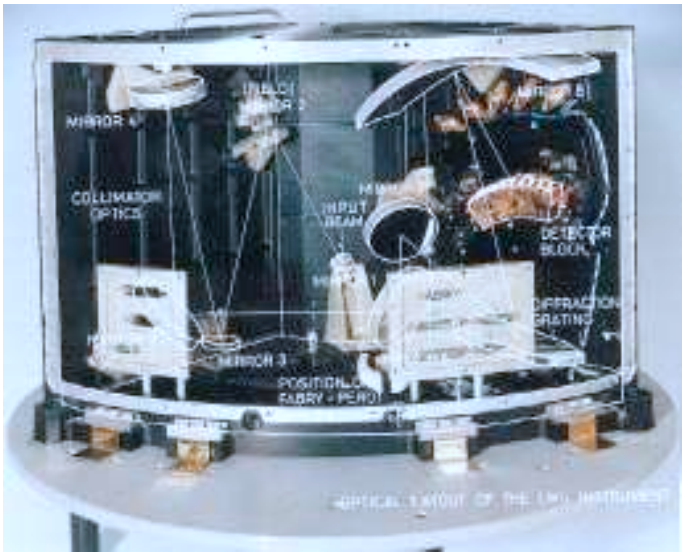

Fig. 1. The optical train of the LWS

2. Description of the Instrument

2.1. Overall design

The LWS consists of three main components, the focal plane unit (FPU), operating at liquid-helium temperatures, and two warm units: the analogue processing unit (APU) - which drives the various mechanisms and powers the detectors in the FPU, as well as processing the resulting signals - and the digital processing unit (DPU), which commands the LWS via the APU and interfaces with the spacecraft data-handling system.

The FPU itself consists of three subsystems: the optical subsystem, the detector subsystem and the Fabry-Perot subsystem. The optical subsystem comprises a collimator, a grating, and refocusing optics which feed the detector subsystem. The Fabry-Perot subsystem, which is situated in the collimated part of the beam, consists of a wheel carrying two Fabry-Perot interferometers. The wheel can be set in any of four positions: in one of these, the beam passes straight through the subsystem whilst in another, the beam is completely obscured. In the remaining two positions, one or other Fabry-Perot is placed in the beam and modulates it spectrally.

2.2. Optical Design (Saisse and Rabou, 1988)

Figure 1 shows the optical train of the LWS superimposed on a photograph of the instrument taken before the integration of the Fabry-Perot subsystem. The f/15 beam from the telescope is folded by mirror (1) and comes to a focus on the mirror (2), which was designed to restrict the field of view on the sky to 1.65 arcmin - the diffraction limit of the telescope at 118 μm. In practice, the beam is somewhat narrower than this (Swinyard et al., 1996). The field mirror is surrounded by a concentric out-of-field rejection mirror to avoid problems with stray light. From mirror (2), the beam passes to the mirrors (3) and (4) before reaching the Fabry-Perot subsystem via the mirror (5). The beam is then reflected by plane mirrors (6) and (7) on to the grating, which has an off-centre Schmidt profile to correct for spherical aberration. Finally, on leaving the grating, the radiation is focused by mirror (8) on to the cylindrical surface of the detector block.

The optical subsystem is designed to satisfy the Jacquinot criterion for the resolution of the instrument, to optimise the collimation of the beam at the position of the Fabry-Perot etalons, and to match the spectral resolution achieved by the instrument in grating mode to the order-sorting needs of the FPs.

The grating is ruled with 7.9 lines per millimetre at a blaze angle of 30^o on a rotationally-symmetric Schmidt profile. It is mounted on a scanning mechanism similar to that used in the SWS and described by de Graauw et al. (1996). With the grating in its rest position, the radiation is incident at an nominal angle of 60^o. The grating is used in second order for the wavelength range $43 - 94.6$ μm and in first order for the wavelength range $94.6 - 196.9$ μm. It can be scanned, by means of a servo-controlled drive mechanism, through $\pm 7.0^o$. The grating was originally intended to scan through $\pm 3.5^o$ in normal operation, a range chosen so that the nominal range of wavelengths covered by one detector channel overlapped that of the adjacent detector by a few micrometers. The extended scanning range of $\pm 7.0^o$ allows - at the cost of a small increase in power dissipated in the focal plane - the nominal wavelength range of any detector channel to be covered by its two neighbours, thus providing redundancy in the case of a failed detector. This increase of the scanning range also extends the long-wavelength coverage out to 196.9 μm. In order to maximise the sensitivity of the instrument at all wavelengths, however, the grating is now scanned more than $\pm 3.5^o$ in normal operation.

2.3. Detectors and Cold Electronics (Church et al., 1993)

Figure 2 is a drawing of the detector block, which contains ten detectors: five of these cover the short-wavelength range $\sim 43 - 90$ μm in nominally 10 μm-wide channels while the others cover the long-wavelength $90 - 197$ μm in nominally

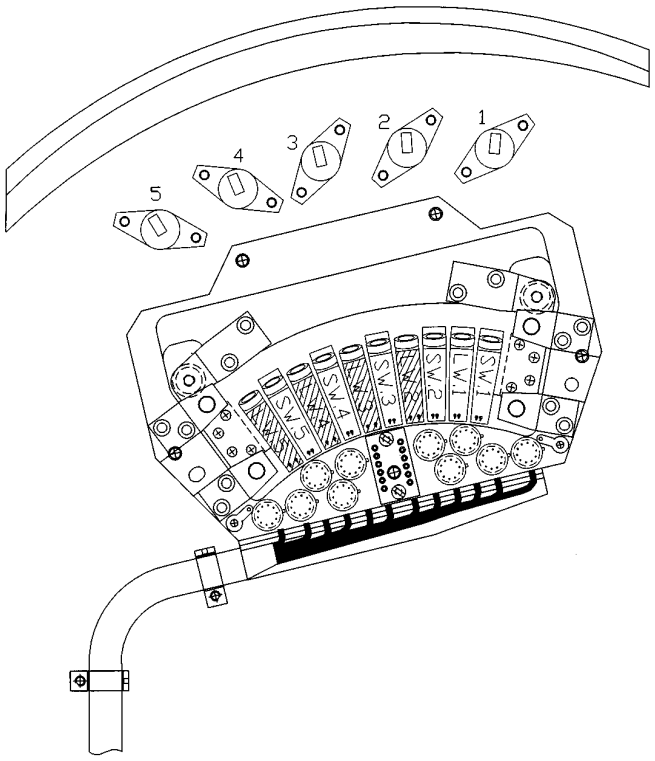

Fig. 2. Drawing of the LWS detector block.

20 μm-wide channels. Radiation in the long-wavelength range - coming from the grating in first order of diffraction - is, of course, focused on to the same range of positions on the detector block as is radiation in the short-wavelength range coming from the grating in the second order of diffraction. Alternate detectors are therefore designed to respond to long and short wavelengths respectively. Consequently, each detector receives not only its "own" wavelength but also other multiples of this wavelength in other orders and must be prevented from responding to these extraneous orders by bandpass filters. This becomes very critical at the shortest wavelengths and makes high demands on the design of the filters.

Three different types of photoconductive detector are used to cover the required range of wavelengths. The shortest wavelength channel SW1 (nominally $43 - 50$ μm) uses a beryllium-doped germanium (Ge:Be) detector. The next five channels in wavelength-space (SW2: $50 - 60$ μm SW3: $60 - 70$ μm, SW4: $70 - 80$ μm, SW5: $80 - 90$ μm and LW1: $90 - 110$ μm) use gallium-doped germanium (Ge:Ga) detectors whilst stressed Ge:Ga is used for the four longest-wavelength channels (LW2: $110 - 130$ μm, LW3: $130 - 150$ μm, LW4: $150 - 170$ μm and LW5: $170 - 190$ μm). [These are the nominal wavelength ranges; the actual range of wavelengths covered by each channel is adjusted to optimise the sensitivity of the instrument at all wavelengths (Swinyard et al., 1996).]

Detectors are mounted in integrating cavities to increase their absorption efficiency and are fed by a horn designed to couple efficiently with the radiation leaving the spherical mirror (8) in figure 1. The stress on the long-wavelength detectors, which is applied with a mechanical screw, reduces the gap between the acceptors and the valence band, thus reducing the energy needed for excitation of carriers into the band. This reduction in energy-gap, however, also allows more carriers to be thermally excited into the band; in order to keep their dark-currents to acceptable levels, therefore, the stressed detectors are operated at the lowest temperature available, that of the helium tank at 1.8 K. The unstressed detectors in contrast, are found to behave poorly at 1.8 K and are therefore operated at 3.0 K. Operating the two types of detector at different temperatures is achieved by mounting them on thermally-separate bars. The unstressed detectors are mounted on the upper of two bars in the detector block. This bar, which accommodates a heater and a thermometer operating in a servo loop, has a weak thermal link to the lower bar. The lower bar, accommodating the stressed detectors (shaded) is thermally shorted to the helium tank with a high-conductance copper strap.

The photo-current in a detector element is accumulated on the input capacitance of an FET in a JF-4 integrating amplifiers supplied by Infrared Laboratories, Inc. These FETs are operated at about 60 K within their TO5 cans, which are carefully shielded to avoid stray thermal emission. The amplifiers are read out at 88 Hz and are re-set at pre-set intervals, usually 0.25 or 0.5 seconds.

Five infrared illuminators, also provided by Infrared Laboratories, Inc., are used to monitor and calibrate the stability of response of the detectors.

2.4. Fabry-Perots (Davis et al., 1995)

For use in high-resolution mode, the LWS contains two Fabry-Perot interferometers mounted on a wheel driven by a pinion engaging gear-teeth on the rim of the wheel: a new type of cryogenic motor was especially developed (Davis et al., 1991) to drive the wheel. The short-wavelength Fabry-Perot covers the wavelength range $47 - 70$ μm whilst the long-wavelength Fabry-Perot deals with the remaining $70 - 196.6$ μm. Rotation of the wheel brings successively into the parallel part of the beam (between mirrors (5) and (6) of figure 1): an open aperture, so that the LWS can be used in moderate-resolution mode as a grating spectrometer; the short-wavelength Fabry-Perot; a blanking plate for measurement of the detectors' dark-currents; and the long-wavelength Fabry-Perot. [In practice, the dark-current is measured with one of the FPs in the beam, its etalon being deliberately made non-parallel to reflect back all radiation arriving via the optical path of the instrument.]

The construction of the Fabry-Perot etalons is shown in figure 3. The moving plate (4) is suspended on leaf-springs (8) between the back plate (1) and the fixed plate (9). Each corner of the moving plate carries a loudspeaker-like drive coil (3) which operates in a gap surrounding a permanent magnet in the back plate (2). The position of each corner, relative to the fixed plate, is determined by measuring the charge on the capacitance micrometer (6), formed by pads on the moving and fixed plates. These positions are controlled by a servo system which supplies

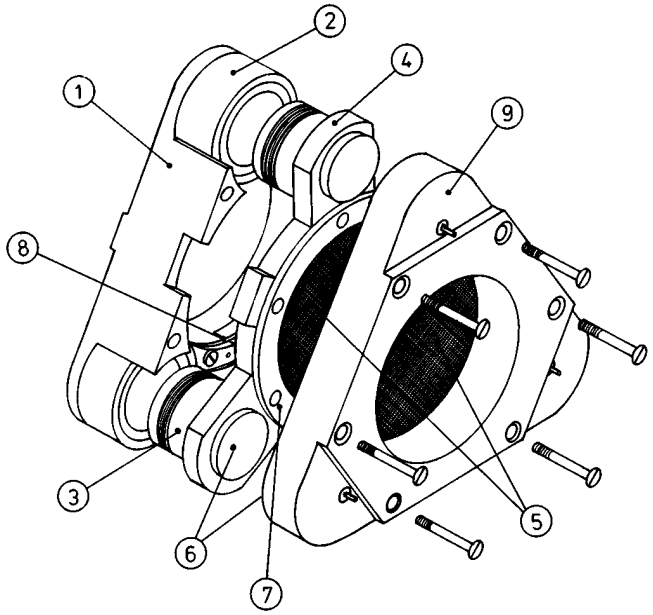

Fig. 3. The construction of a Fabry-Perot etalon.

sufficient current to the drive coil to make the measured charge equal to a control value. The two plates are scanned parallel to each other by applying appropriate signals to the three coils.

The fixed and moving plates carry the reflecting elements (5), made of free-standing nickel meshes supplied by Heidenhain; these meshes are affixed to the mesh-mounting rings (7) which are attached to the plates. The meshes consist of a rectangular grid of rectangular section: the thickness of the meshes is 3 μm, the width of the "bars" of which the meshes are composed is 6 μm, and the periods of the grid are 19 μm for the long-wavelength Fabry-Perot and 15.5 μm for the short-wavelength Fabry-Perot. The narrow tolerance allowed on these dimensions is critical to the performance of the instrument.

3. Using the LWS Instrument (Clegg et al., 1994)

3.1. Summary

The LWS has two operational modes: grating (medium-resolution) mode and Fabry-Perot (high-resolution) mode. It has six different observational modes which can be accessed via four Astronomical Observation Templates (AOTs, cf. section 3.3).

3.2. Operational Modes of the Instrument

3.2.1. Grating Mode

In grating mode, the Fabry-Perot wheel is turned to its open position and the grating is scanned over the range of angle needed to cover the desired wavelength range. Note that, all detectors are receiving radiation all the time and the corresponding data are being read out. Whether or not these data are useful to the observer depends upon the range of wavelengths selected. The software used to implement the AOTs, however, make use of this multiplexing where possible to minimise the length of scan and therefore the time needed to carry out an observation. The spectral resolution elements in grating mode are 0.29 μm in the short-wavelength channels (SW1 - SW5) and 0.60 μm in the long-wavelength channels (LW1 - LW5). These resolution elements correspond to a resolving power ranging between about 150 and 300.

3.2.2. Fabry-Perot Mode

In Fabry-Perot mode, the grating is moved so as to maximise the power falling on the detector at the wavelength under investigation and the appropriate Fabry-Perot is used to scan about that wavelength. If a range of wavelengths is to be studied, the grating will be moved periodically so as to keep the grating transmission as near maximum as possible. Although multiplexing between detectors still occurs - radiation in different orders of the Fabry-Perot will be falling on detectors other than the one selected for the wavelength of interest - it is unlikely that any of these data will be useful. There are two reasons for this. First, there may not be spectral lines in the other orders. Secondly, and more importantly, the grating will be set so that it has peak transmission at the Fabry-Perot order of interest. Other orders will fall on the (uncalibrated) wings of the grating's spectral response function.

The resolving power achieved in Fabry-Perot mode varies between 6800 and 9700. The free spectral range of a Fabry-Perot is given by λ/n, where n is the order of interference. Its resolving power, on the other hand is given by nF, where F is its finesse. In order to achieve a resolving power of 10^4 with the available finesses of about 100, we need to operate in orders of around 100; the ratio of the wavelength to the free spectral range is then also about 100. If the grating is to avoid spectral contamination, by preventing adjacent spectral orders of the Fabry-Perots from reaching the detectors, its resolving power must therefore also be about 100. It was the need for the grating to order-sort for the Fabry-Perot which set the requirement on the resolving power of the grating. In both grating and Fabry-Perot modes, observations are carried out with one of two standard lengths of detector integration ramps, 0.25s and 0.5s. The total integration time per spectral point is then achieved by varying the number of these ramps. It was originally intended that spectra be obtained by carrying out a number of integrations at each setting of the grating or Fabry-Perot until the total required integration time had been built up. In order to minimise the low-frequency end of 1/f noise, however, a fast-scanning mode was also implemented. In this mode, only one integration is performed at each position of the grating or Fabry-Perot, the total integration time being built up by repeated scanning. This method is now recommended for all observations because it avoids successive integration ramps being affected by the same particle hit (cf. Swinyard et al., 1996).

3.3. Observational Modes of the Instrument

3.3.1. Medium-Resolution Wavelength Range LWS01

This grating-mode AOT results in a medium-resolution spectrum covering a wavelength range, specified by the user, up to the full range of the LWS in medium-resolution mode ($43.0 - 196.9$ μm). There is a minimum to the range covered, corresponding to 1.25 μm for the short-wavelength channels (SW1 - SW5) and 2.5 μm for the long-wavelength channels (LW1 - LW5). Data are recorded from all ten detectors while the specified range is being scanned. The observer has a choice of sampling the spectrum at 1, 1/2 or 1/4 of a resolution element.

3.3.2. Medium-Resolution Line Spectrum LWS02

This AOT produces medium-resolution spectra around up to 10 wavelengths, specified by the observer. Data are recorded from all ten detectors while the specified ranges are being scanned. The observer has a choice, in fractions of a resolution element, of the spectral sampling interval.

3.3.3. High-Resolution Wavelength Range LWS03

This AOT results in a high-resolution spectrum covering a wavelength range, specified by the user, up to the full range of the LWS ($47.0 - 196.6$ μm) in high-resolution mode. Useful data are recorded from only one detector at a time. The observer has a choice of sampling the spectrum at 1, 1/2 or 1/4 of a resolution element.

3.3.4. High-Resolution Line Spectrum LWS04

This AOT produces high-resolution spectra around up to 10 wavelengths, specified by the observer. Useful data are recorded from only one detector at a time. The observer has a choice of sampling the spectrum at 1, 1/2 or 1/4 of a resolution element.

3.3.5. Narrow-Band Photometry LWS02

In this mode, the grating is not scanned but kept at a fixed position by a special choice of a parameter in AOT LWS02. The result is narrow-band photometry at ten wavelengths, determined by the choice of a single wavelength, within the range $43 - 196.9$ μm. The spectral resolution element is 0.29 μm in the short-wavelength channels (SW1 - SW5) and 0.60 μm in the long-wavelength channels (LW1 - LW5).

3.3.6. Serendipitously Parallel Mode

Long after the design of the instrument and its observing modes was complete, it was realised that a limited number of astronomically useful data could be transmitted in housekeeping channels while the satellite was slewing or other instruments were being used. In this mode, the slope of the integration ramps is simply estimated on board by taking the difference between a sample at the beginning and end of the ramp. Moreover, because there is none of the usual monitoring of changes in detector responsivity or dark-current (cf. Swinyard et al., 1996), the accuracy with which the signals are extracted is significantly reduced. Lastly, the data cannot be processed by standard methods. For all these reasons, the mode is available only to members of the LWS Consortium.

4. Conclusion

The Long-Wavelength Spectrometer was designed to provide astronomers with a spectroscopic tool in a region of the electromagnetic spectrum largely inaccessible hitherto. It is fully functioning in orbit and is producing spectra from a variety of astronomical objects: other papers in the volume illustrate the results being achieved.

Acknowledgements. The LWS was designed and built by a consortium of scientists and engineers from Canada, France, Italy, the UK and the USA. Hardware and software were provided by: Centre d'Etude Spatiale des Rayonnements, Toulouse, France; Istituto de Fisica dello Spazio Interplanetario, Frascati, Italy; Laboratoire Astronomie Spatiale, Marseille, France; Mullard Space Science Laboratory, University College London, Holmbury St Mary, UK; Rutherford Appleton Laboratory, Chilton, UK; Queen Mary and Westfield College, London, UK; University College London, London, UK. The authors gratefully acknowledge funding by the following national agencies: CNES, CNR, NASA, NSERC and PPARC.

References

Church, S.E., Griffin, M.J., Ade, P.A.R., Price, M.C., Emery, R.J. and Swinyard, B.M., 1996, Infrared Physics 34, 389

Clegg, P.E., Heske, A. and Trams, N.R., 1994. LWS/PEC/2039.01 "Observers's Manual", Issue 1

Davis, G.R., Furniss, I., Towlson, W.A., Ade,P.A.R., Emery, R.J., Glencross, W.M., Naylor, D.A., Patrick, T.J., Sidey, R.C and Swinyard, B.M., 1995, Appl. Optics, 34, 92

de Graauw, Th, et al., 1996. This issue.

Kessler, M.F. et al., 1996. This issue.

Davis,G.R., Furniss,I., Patrick,T.J., Sidey.R.C. and Towlson,W.A. 1991. In 25th Aerospace Mechanisms Symposium, Pasadena, May. NASA conference publication 3113

Saisse, M. and Rabou, P. 1998. In SPIE vol. 1013, "Opitcal Design Methods and Large Optics", pp 66-73.

Swinyard et al., 1996. This issue.